Biosynthesis of Zinc Oxide Nanoparticles from *Schrebera swietenioides* Roxb. Leaves Extract and their Potent Photocatalytic Activities

S. Lakshmi Tulasi[1,*,] , P. Sumalatha[2,] , Shaheda Niloufer[3,] , P. Pavani[1,] and N. Usha Rani[1,]

[1]Department of Freshman Engineering, PVP Siddhartha Institute of Technology, Kanuru, Vijayawada-520007, India
[2]Department of Basic Sciences and Humanities, Seshadri Rao Gudlavalleru Engineering College, Gudlavalleru-521356, India
[3]Department of Freshman Engineering, Lakireddy Bali Reddy College of Engineering, Mylavaram-521230, India

*Corresponding author: E-mail: tulasi13111986@gmail.com

Zinc oxide nanoparticles was synthesized using from *Schrebera swietenioides* Roxb. leaves extract. The size, shape, surface morphology, functional groups and chemical composition of the aqueous extracts mediated zinc nanoparticles was evaluated using various characterization techniques. The UV-visible absorption spectra shows the characteristic maximum absorption at 379 nm, which confirmed its narrow size distribution and mono-dispersed nanoparticles. The SEM analysis confirmed that the particles were more or less spherical in shape with rough surfaces having the particle size in the range of 54 nm to 97 nm. The EDS analysis confirmed the presence of zinc at 8.61 keV (Kα) and 1.09 keV (Lα), whereas the XRD spectra shows the 2θ characteristic peaks corresponds to planes as same as the crystal lattice structure. The biosynthesized ZnO nanoparticles have excellent tendency to degrade methyl orange and crystal violet dyes, which was achieved within 2 h.

Keywords: Zinc oxide Nanoparticles, Plant extract, Photocatalytic reduction, Methyl orange dye, Crystal violet dye.

INTRODUCTION

Overcoming the challenges caused by numerous environmental pollutants, plants are seen as cost-effective and eco-friendly chemical sources. They also have the ability to detoxify heavy metals [1]. The synthesis of nanoparticles using plant extracts considered as clean and environmentally accepted "Green Chemistry" concept [2]. The synthesis of nanoparticles using plant extracts has considerable advantage than the synthesis through microorganisms due to involvement of complex process of preserving the microbial strains as well as maintaining the culture without contamination. Nanoparticles derived from plant extracts had a reaction kinetics which is on the same level with chemically generated nanoparticles [3]. Due to the high quantities of phytochemicals in plant components *viz.*, seeds, fruits, leaves, stems, bark, roots, *etc.* such components are utilized in the synthesis of nanoparticles [4,5].

Pulit-Prociak *et al.* [5] reported that the ZnO nanoparticles has drawn high interest due to its wide range of applications in various fields such as optics, electronics and biomedical systems.

These nanoparticles were enlisted as "generally recognized as safe" by US FDA. These nanoparticles have high exciton binding energy (60 meV) and high band gap (3.37 eV) that implies tremendous semiconducting properties. These nanoparticless also have anti-inflammatory, wound healing, optic, UV filtering and high catalytic activity [6,7]. ZnO nanoparticles have significant UV filtering activity and hence are widely used in preparing various cosmetics such as sunscreen lotions for protecting skin from UV light [8]. The reported studies confirm that green synthesized ZnO nanoparticles exhibit various shapes such as nanowire, nanobelt, nanorod, nanoflower, nanoflakes, *etc.* [9].

Numerous findings summarized that the green synthesized nanoparticles having high efficiency on the degradation of various dyes and have proved to be having excellent organic pollutants degradation efficiency [10]. The nanoadsorbents were proved to be having remarkable efficiency in pollutant removal from wastewater, however, due to the presence of high number of nanoparticles were involved in the pollutant removal there may be a chance of residual nanoparticles toxicity in the treated water [11].

EXPERIMENTAL

The analytical reagent grade chemicals used in the study such as zinc acetate dihydrate, sodium hydroxide, hydrogen peroxide, dibasic disodium phosphate, monobasic sodium dihydrogen phosphate, methyl orange, crystal violet were purchased from Merck Chemicals and SD Fisher Scientific, Mumbai, India.

Collection of plant material: The leaves of *Schrebera swietenioides* Roxb. was collected from the hilly area located in Tirumala (13.6807º N, 79.3509º E), Tirupati, India. The collected plant sample was authenticated by Dr. Ch. Srinivasa Reddy, Assist. Prof, Department of Botany, SRR & CVR Government Degree College (A) Vijayawada, India with plant authentication no. SRR-CVR/2019-20/Bot/31. The collected leaves of plant were thoroughly cleaned to remove the sand and dirt using sterile cotton followed by double distilled water.

Extraction of plant: An accurately weighed 10 g of dried leaves powder was added in 100 mL of double distilled water and then boiled the solution on a hot plant at 40 ºC for 80 min. The phytochemical constituents present in the plant material were extracted to the water solvent [12]. Then the extract was filtered, the plant material obtained as sediment was discarded and the clear filtrate was made up to 100 mL with distilled water. The clear filtrate obtained was preserved for the further studies synthesis of nanoparticles.

Green synthesis of ZnO nanoparticles: The zinc oxide nanoparticles was synthesized by utilizing aqueous leaf extract of *S. swietenioides* and zinc acetate solution [13]. The aqueous leaf extract and zinc acetate solution in 10:90 (v/v) was mixed and the homogenous mixture was prepared by stirring the solution in a magnetic stirrer for 4 h without heating. Then 20 mL of ethanolic NaOH solution was added and stirred for 5 min. The settled precipitated $Zn(OH)_2$ was collected by removing the excess mother liquid through filteration and then washed with excess distilled water to remove the extract particles on the precipitate. The obtained solid product $Zn(OH)_2$ was converted in to powdered ZnO nanoparticles by heating at 300 ºC for 45 min in a muffle furnace.

Characterization: The size, shape, surface morphology, functional groups and the chemical composition of *Schrebera swietenioides* aqueous leaves extracts mediated zinc oxide nanoparticles was evaluated using various characterization techniques. The nanoparticle solution was scanned in the UV visible spectral range of 800-200 nm range using UV-Vis spectrophotometer (Avantes Avalight-DH-5-BAL) instrument. The identification of the functional groups and phytochemicals in the leave extract was obtained by FTIR spectroscopy within the 4000-500 cm^{-1} range using Nicolet FT-IR Spectrometer 5700 instrument. In order to investigate the surface topography and compositions of ZnO nanoparticles, scanning electron microscopy (JSM-JEOL 6390 Scanning Electron Microscope) was utilized. The elemental composition of *S. swietenioides* aqueous leave extract mediated zinc nanoparticle was evaluated by X-ray spectroscopy (EDX) analysis, which was performed on Shimadzu DX-700HS instrument. The shape and size of *S. swietenioides* aqueous leaves extract mediated zinc and copper

nanoparticles was evaluated by performing TEM analysis using JEOL model JEM-1010, Tokyo, Japan. The XRD analysis (XRD) was performed in the scan range of 20º to 80º diffraction angles (2θ) at 2º/min scan speed using X'pert PRO PANalytical diffractmeter.

RESULTS AND DISCUSSION

The present work focused on the green synthesis of zinc oxide using aqueous leaves extract of *Schrebera swietenioides* Roxb. Further the synthesized ZnO nanoparticles were evaluated for its photocatalytic activity for the reduction of toxic dyes. The preliminary conformation of the formation of ZnO nanoparticles in the reaction solution was carried by scanning the solution in the UV-visible spectrophotometer. The UV-visible absorption spectrum exhibit the characteristic maximum absorption wavelength peak at 379 nm confirms its narrow size distributed and mono-dispersed nanoparticles (Fig. 1). The FT-IR analysis of the green synthesized nanoparticles shows the involvement of several bioactive functional groups in the formation of ZnO nanoparticles. The FT-IR spectrum of ZnO nanoparticles (Fig. 2) shows the signals corresponds to free -OH in alcohols at 3668 cm^{-1}, the O-H stretching in intramolecular bonded alcohols at 3461 cm^{-1}, the N-H stretching in amine salts at 3000-2800 cm^{-1}, the C-H stretching in alkanes at 3005 cm^{-1}), the C-H bending in aromatic compounds at 1655 cm^{-1}, the C-N stretching at 1314 cm^{-1} and the C-O stretching due to the aromatic esters at 1287 cm^{-1} were observed.
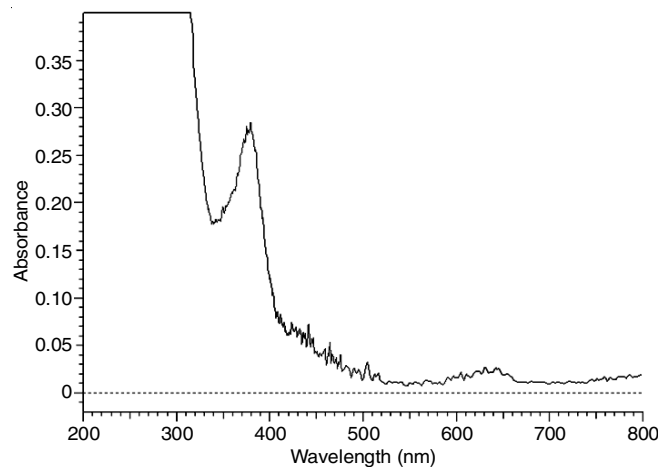
Fig. 1. UV-visible absorption spectra of zinc oxide nanoparticles
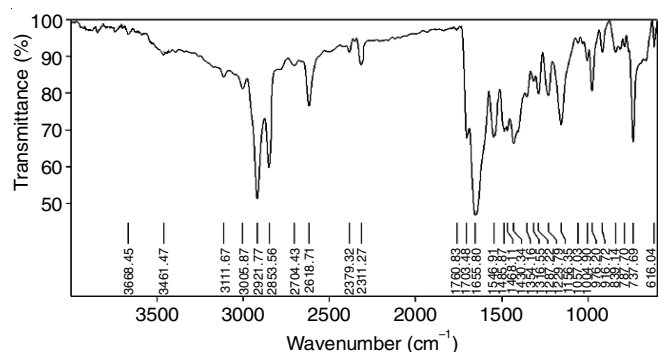
Fig. 2. FT-IR spectrum of zinc oxide nanoparticles synthesized using aqueous leaf extract of *S. swietenioides*

The SEM analysis of the synthesized ZnO nanoparticles confirmed that the nanoparticles were more or less spherical in shape with rough surfaces having the particle size in the range of 54 nm to 97 nm (Fig. 3). The EDS analysis further confirmed the presence of zinc at 8.61 keV (Kα) and 1.09 keV (Lα). The peak corresponds to oxygen was identified at 0.5 keV. The elemental analysis proved that the nanoparticles show the 73.7% of the metallic zinc content (Fig. 4). Similarly, using TEM technique, the size and shape of the green synthesized ZnO nanoparticles were also examined and the results are shown in Fig. 5 which range from 58 to 100 nm. The majority of the nanoparticles had nearly consistent sizes and the average mean of 75 nm. Based on these results, leaves extract could be a useful reducing and capping agent. The XRD spectra of the ZnO nanoparticles synthesized using aqueous leaves extract of *S. swietenioides* shows the 2θ characteristic peaks corresponds to planes as same as the crystal lattice structure (Fig. 6). The peaks identified at 2θ value of 31.60º, 34.22º, 36.11º, 47.35º, 56.45º, 62.69º, 66.11º, 67.84º, 68.87º, 71.70º and 76.64º, which corresponds to 100, 002, 101, 102, 110, 103, 200, 112, 201, 004 and 202 planes of the crystal lattice. The current findings is consistent with previous research that demonstrated the hexagonal wurtzite structure of ZnO-nanoparticles [14].
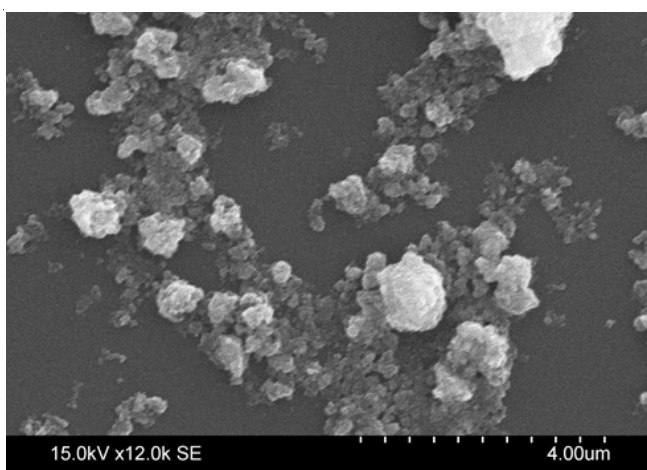
Fig. 3.   SEM image of the aqueous leaf extract of *S. swietenioides* mediated zinc oxide nanoparticles
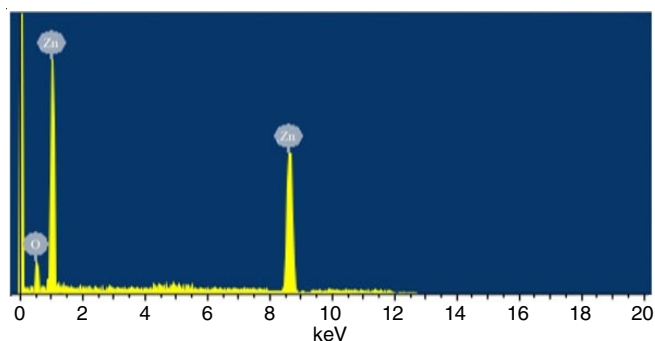
Fig. 4.   EDS spectra of the aqueous leaf extract of *S. swietenioides* mediated zinc oxide nanoparticles

Fig. 5.   TEM micrograph of the aqueous leaf extract of *S. swietenioides* mediated zinc oxide nanoparticles
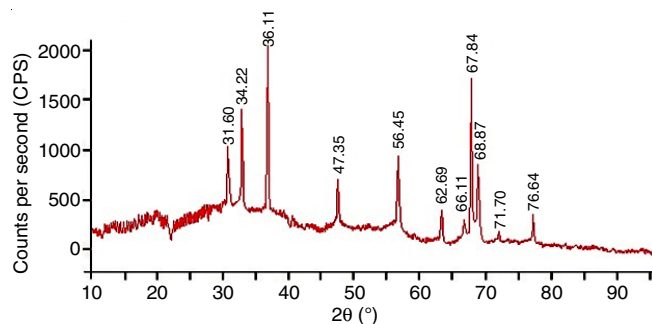
Fig. 6.   XRD spectrum of the aqueous leaf extract of *S. swietenioides* mediated zinc oxide nanoparticles

Photocatalytic reduction of methyl orange dye: The reduction study was performed at various dosage of ZnO nanoparticles at the optimized 50 ppm concentration of methyl orange dye. The results confirmed that photocatalytic activity increased with increase in dose of the ZnO nanoparticles. Table-1 presents the results of a study on the degradation of methyl orange dye

	TABLE-1			
	REDUCTION STUDY OF METHYL ORANGE AT VARIOUS STRENGTHS OF *S. swietenioides* MEDIATED ZINC OXIDE NANOPARTICLES			
Time (min)	% of Methyl orange reduction at nanocatalyst strength			
	0.25 g/L	0.50 g/L	0.75 g/L	1.0 g/L
15	12.11 ± 0.076	16.71 ± 0.035	21.78 ± 0.282	38.45 ± 0.067
30	21.28 ± 0.070	29.66 ± 0.106	39.75 ± 0.112	49.61 ± 0.045
45	32.58 ± 0.061	37.85 ± 0.057	56.84 ± 0.085	67.46 ± 0.112
60	41.62 ± 0.040	48.55 ± 0.052	75.79 ± 0.156	86.82 ± 0.095
75	49.27 ± 0.100	57.64 ± 0.042	79.87 ± 0.075	92.51 ± 0.070
90	52.27 ± 0.076	66.43 ± 2.927	82.43 ± 0.251	93.21 ± 0.071
105	53.22 ± 0.031	69.21 ± 0.040	83.65 ± 0.035	94.19 ± 0.085
120	54.16 ± 0.081	69.68 ± 0.266	84.50 ± 0.074	95.14 ± 0.036

using different amounts of green syntheszied ZnO nanoparticles. The % degradation efficiency at 60 min was observed to be 41.62 ± 0.040, 48.55 ± 0.052, 75.79 ± 0.156 and 86.82 ± 0.095%, respectively at the dosage of 0.25, 0.50, 0.75 and 1.0 g/L. However, if the time increase, then the degradation was further continued up to 2 h and the % degradation efficiency was found to be 54.16 ± 0.081, 69.68 ± 0.266, 84.50 ± 0.074 and 95.14 ± 0.036, respectively. The confirmation of the reduction was further confirmed by comparing the UV-visible absorption spectra of methyl orange dye before and after treatment with the ZnO nanoparticles as shown in Fig. 7.
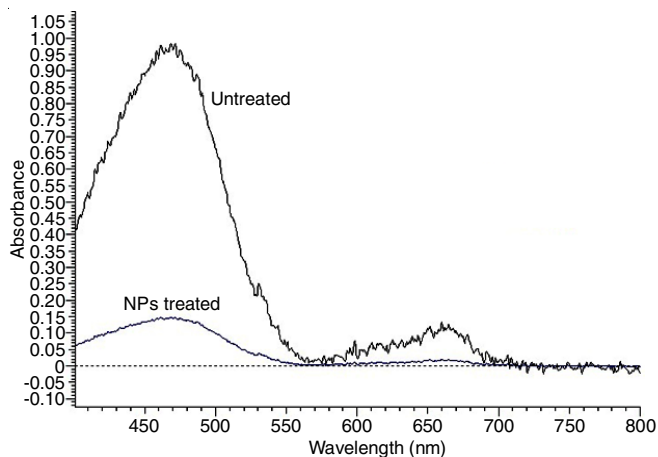
Fig. 7.   Comparative UV visible absorption spectra of before and after nanoparticles treated methyl orange solution

The rate constant of the catalytic degradation of methyl orange dye using the synthesized ZnO nanoparticles was assessed by plotting the graph by considering the time of reduction on *x*-axis and $\ln(A_o/A_t)$ on *y*-axis (Fig. 8). The results confirmed that the degradation of methyl orange dye using ZnO nanoparticles follows the pseudo first-order reaction mechanism for all the dosage of photocatalytic material.

Photocatalytic reduction of crystal violet dye: The reduction study was performed at various dosage of green synthesized ZnO nanoparticles and at the optimized 10 ppm concentration of crystal violet dye. The reduction efficiency was also observed to be increase with increase in contact time. Table-2 shows the degradation data of the crystal violet dye at various dosage of ZnO nanoparticles. The degradation efficiency was observed to be high in the initial time and the maximum degra-
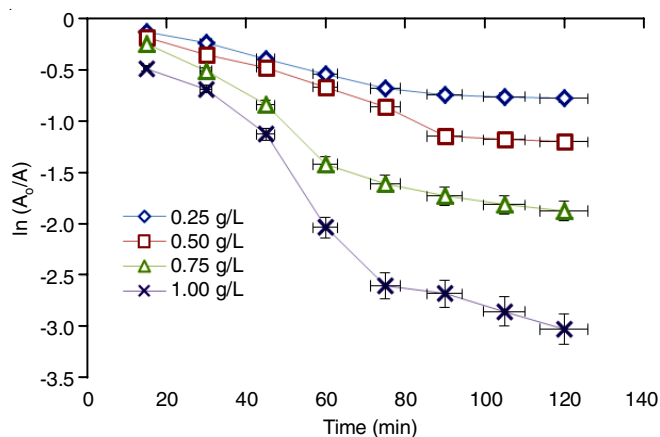
Fig. 8. Photodegradation time profile of A_t/A_o for methyl orange dye

dation was completed within 60 min of time. The % degradation efficiency at 60 min was observed to be 85.33 ± 0.02, 76.36 ± 0.03, 37.82 ± 0.170 and 26.49 ± 0.199%, respectively at the dose of 1.0, 0.75, 0.50 and 0.25 g/L. The reduction time was continued further continue up to 2 h and the % degradation was observed as 94.90 ± 0.031, 81.95 ± 0.035, 48.94 ± 0.042 and 31.61 ± 0.060, respectively. Fig. 9 displays the pre- and post-treatment UV-visible absorption spectra of crystal violet dye treated with ZnO nanoparticles.
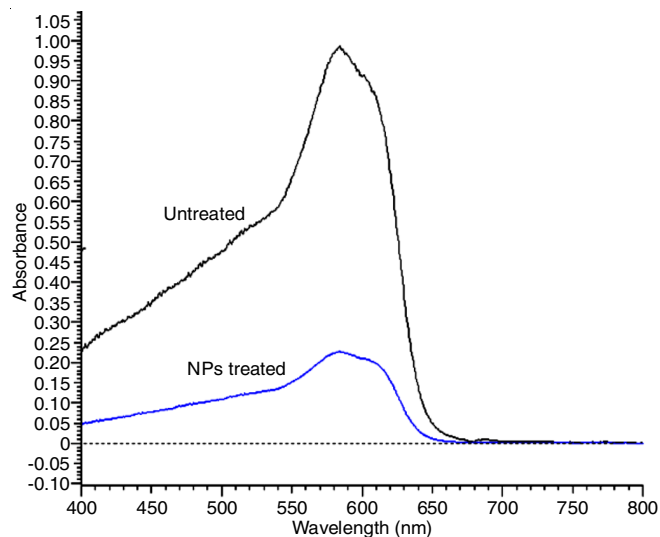
Fig. 9.   Comparative UV visible absorption spectra of before and after nanoparticles treated crystal violet solution

TABLE-2
REDUCTION STUDY OF CRYSTAL VIOLET AT VARIOUS STRENGTHS
OF *S. swietenioides* MEDIATED ZINC OXIDE NANOPARTICLES

Time (min)	% of Crystal violet reduction at nanocatalyst strength			
	0.25 g/L	0.50 g/L	0.75 g/L	1.0 g/L
15	11.31 ± 0.208	15.60 ± 0.082	37.84 ± 0.101	44.67 ± 5.421
30	19.43 ± 0.135	23.87 ± 0.110	49.58 ± 0.055	57.86 ± 0.061
45	24.38 ± 0.226	31.74 ± 0.100	66.22 ± 0.030	74.41 ± 0.065
60	26.49 ± 0.199	37.82 ± 0.165	76.36 ± 0.025	85.33 ± 0.020
75	29.55 ± 0.104	47.84 ± 0.096	79.22 ± 0.071	92.28 ± 0.060
90	30.16 ± 0.076	47.57 ± 0.067	80.11 ± 0.020	93.12 ± 0.040
105	31.03 ± 0.050	47.97 ± 0.093	81.09 ± 0.072	94.11 ± 0.025
120	31.61 ± 0.060	48.94 ± 0.042	81.95 ± 0.035	94.90 ± 0.031

The rate constant of the catalytic degradation of crystal violet dye was also assessed by plotting the graph by considering the time of reduction in minutes and $\ln(A_o/A_t)$ (Fig. 10). The results confirmed that the degradation of crystal violet dye using ZnO nanoparticles follows the pseudo first-order reaction mechanism for all the dosage of ZnO nanoparticles.
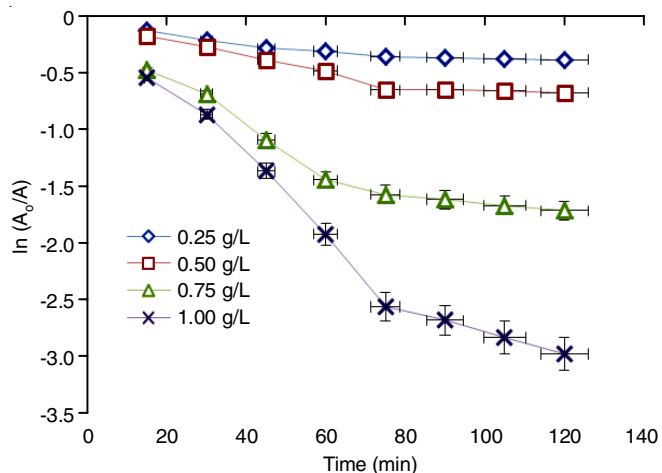
Fig. 10. Photodegradation time profile of A_t/A_o for crystal violet dye

Conclusion

Finally, it can be concluded that the study reports the green synthesis of zinc nanoparticles using aqueous leaf extract of *Schrebera swietenioides* Roxb. The synthesized nanoparticles were characterized and proved that the particles synthesized in the study were in nanosized particles having high % composition of Zn content. The synthesized ZnO nanoparticles were effective in the photocatalytic degradation of various toxic dyes.

CONFLICT OF INTEREST

The authors declare that there is no conflict of interests regarding the publication of this article.

REFERENCES

1. M. Shahid, C. Dumat, S. Khalid, E. Schreck, T. Xiong and N.K. Niazi, *J. Hazard. Mater.*, **325**, 36 (2017);
https://doi.org/10.1016/j.jhazmat.2016.11.063

2. K. Pal, S. Chakroborty and N. Nath, *Green Process. Synth.*, **11**, 951 (2022);
https://doi.org/10.1515/gps-2022-0081

3. S. Iravani, *Green Chem.*, **13**, 2638 (2011);
https://doi.org/10.1039/c1gc15386b

4. H. Agarwal, S. Venkat Kumar and S. Rajeshkumar, *Resource-Effic. Technol.*, **3**, 406 (2017);
https://doi.org/10.1016/j.reffit.2017.03.002

5. J. Pulit-Prociak, J. Chwastowski, A. Kucharski and M. Banach, *Appl. Surf. Sci.*, **385**, 543 (2016);
https://doi.org/10.1016/j.apsusc.2016.05.167

6. S.V. Gudkov, D.E. Burmistrov, D.A. Serov, M.B. Rebezov, A.A. Semenova and A.B. Lisitsyn, *Front. Phys.*, **9**, 641481 (2021);
https://doi.org/10.3389/fphy.2021.641481

7. S. Raha and M. Ahmaruzzaman, *Nanoscale Adv.*, **4**, 1868 (2022);
https://doi.org/10.1039/D1NA00880C

8. J. Jiang, J. Pi and J. Cai, *Bioinorg. Chem. Appl.*, **2018**, 1062562 (2018);
https://doi.org/10.1155/2018/1062562

9. H. Agarwal, S.V. Kumar and S. Rajeshkumar, *Resource-Efficient Technol.*, **3**, 406 (2017);
https://doi.org/10.1016/j.reffit.2017.03.002

10. V. Batra, I. Kaur, D. Pathania, Sonu and V. Chaudhary, *Appl. Surf. Sci. Adv.*, **11**, 100314 (2022);
https://doi.org/10.1016/j.apsadv.2022.100314

11. P.C. Nagajyothi, S.V. Prabhakar Vattikuti, K.C. Devarayapalli, K. Yoo, J. Shim and T. V. M. Sreekanth, *Crit. Rev. Environ. Sci. Technol.*, **50**, 2617 (2020);
https://doi.org/10.1080/10643389.2019.1705103

12. L. Dong, L. Han, T. Duan, S. Lin, J. Li and X. Liu, *RSC Adv.*, **10**, 2027 (2020);
https://doi.org/10.1039/C9RA07799E

13. S.W. Balogun, O.O. James, Y.K. Sanusi and O.H. Olayinka, *SN Appl. Sci.*, **2**, 504 (2020);
https://doi.org/10.1007/s42452-020-2127-3

14. S.-Y. Pung, W.-P. Lee and A. Aziz, *Int. J. Inorg. Chem.*, **2012**, 608183 (2012);
https://doi.org/10.1155/2012/608183